Centrum voor Wiskunde en Informatica
Centre for Mathematics and Computer Science

M.H. Lallemand, B. Koren

Iterative defect correction and multigrid accelerated explicit time stepping schemes for the steady Euler equations

Department of Numerical Mathematics Report NM-R8908 April

The Centre for Mathematics and Computer Science is a research institute of the Stichting Mathematisch Centrum, which was founded on February 11, 1946, as a nonprofit institution aiming at the promotion of mathematics, computer science, and their applications. It is sponsored by the Dutch Government through the Netherlands Organization for the Advancement of Research (N.W.O.).

Iterative Defect Correction and Multigrid Accelerated Explicit Time Stepping Schemes for the Steady Euler Equations

Marie-Hélène Lallemand
INRIA Sophia-Antipolis
Route des Lucioles, 06565 Valbonne, France
present address:
Computational Mathematics Group
Campus Box 170, University of Colorado at Denver
1100 14th Street, Denver, Colorado 80202, U.S.A.

Barry Koren
CWI
Kruislaan 413, 1098 SJ Amsterdam, The Netherlands

Analytical and experimental convergence results are presented for a new pseudo-unsteady solution method for second-order accurate upwind discretizations of the steady Euler equations. Comparisons are made with an existing pseudo-unsteady solution method. Both methods make use of nonlinear multigrid for acceleration and nested iteration for the fine grid initialization. The new method proposed follows a less direct approach than the existing one. It uses iterative defect correction. Analysis shows that it has better stability and smoothing properties. The analytical results are confirmed by numerical experiments. The new method leads to both better convergence and efficiency.

1980 Mathematics Subject Classification: 65B05, 65N10, 65N20, 65N30, 65N40, 76G15.
Keywords and Phrases: defect correction, multigrid, explicit time stepping, Euler equations
Note: This work was performed in the framework of a cooperation between l'Institut National de Recherche en Informatique et en Automatique (INRIA) and het Centrum voor Wiskunde en Informatica (CWI). The investigations were supported in part by le Centre National d'Etudes Spatiales (CNES).

1. Introduction

1.1. Equations

The equations considered are the steady, 2D, compressible Euler equations

$$\frac{\partial F(W)}{\partial x} + \frac{\partial G(W)}{\partial y} = 0, \tag{1.1}$$

where

$$W = \begin{bmatrix} \rho \\ \rho u \\ \rho v \\ \rho e \end{bmatrix}, \quad F(W) = \begin{bmatrix} \rho u \\ \rho u^2 + p \\ \rho uv \\ \rho u(e + p/\rho) \end{bmatrix}, \quad G(W) = \begin{bmatrix} \rho v \\ \rho uv \\ \rho v^2 + p \\ \rho v(e + p/\rho) \end{bmatrix}. \tag{1.2}$$

Assuming a perfect gas, the total energy e satisfies $e = p/(\rho(\gamma-1)) + \frac{1}{2}(u^2+v^2)$. The ratio of specific heats γ is assumed to be constant.

Report NM-R8908
Centre for Mathematics and Computer Science
P.O. Box 4079, 1009 AB Amsterdam, The Netherlands

1.2. Spatial discretization

The geometrical partitioning is hybrid. To handle complex geometries, as basic partitioning, a finite element triangularization is used. The partitioning may be unstructured. For the actual computation, from this, a finite volume partitioning is derived with as volume vertices the barycentres of the triangular elements. For details about this dual gridding we refer to [1,9]. Given an unstructured triangularization, the finite volume grid is inherently unstructured as well.

For all finite volumes C_i, $i=1,2,\ldots,n_i$, we consider the integral form

$$\oint_{\partial C_i} \{F(W)n_x + G(W)n_y\}\,ds = 0, \quad i=1,2,\ldots,n_i. \tag{1.3}$$

For the Euler equations, because of their rotational invariance, (1.3) may be rewritten as

$$\oint_{\partial C_i} T(n_x,n_y)F(W)ds = 0, \quad i=1,2,\ldots,n_i, \tag{1.4}$$

where $T(n_x,n_y)$ is the rotation matrix

$$T(n_x,n_y) = \begin{bmatrix} 1 & 0 & 0 & 0 \\ 0 & n_x & n_y & 0 \\ 0 & -n_y & n_x & 0 \\ 0 & 0 & 0 & 1 \end{bmatrix}. \tag{1.5}$$

For simplicity, for all $i=1,2,\ldots,n_i$ we assume the flux $F(W)$ to be constant along each (bi- or multi-) segment $\partial C_{i,j}$ of the volume boundary ∂C_i, $\partial C_{i,j} \equiv C_i \cap C_{i,j}$, $C_{i,j}$ being a neighbouring volume of C_i. (Thus $\partial C_i = \cup \partial C_{i,j}$, $j=1,2,\ldots,n_{i,j}$, with $n_{i,j}$ the number of volumes $C_{i,j}$.) Introducing - following [9] - a straight path $\partial \bar{C}_{i,j}$ related to $\partial C_{i,j}$, (1.4) can be simplified to

$$\sum_{j=1}^{n_{ij}} T(\bar{n}_x,\bar{n}_y)_{i,j} F(W)_{i,j} \bar{l}_{i,j} = 0, \quad i=1,2,\ldots,n_i, \tag{1.6}$$

where $(\bar{n}_x,\bar{n}_y)^T$ and $\bar{l}_{i,j}$ are the outward unit normal and the length of this particular path, respectively.

Crucial and still free in (1.6) is the way of evaluating $F(W)_{i,j}$. For this we use an upwind scheme which may be any scheme from the family of well-known upwind schemes [17,12,14,16]. With this, (1.6) can be rewritten as

$$\sum_{j=1}^{n_{ij}} T(\bar{n}_x,\bar{n}_y)_{i,j}\, \Phi(W^l_{i,j}, W^r_{i,j})\, \bar{l}_{i,j} = 0, \quad i=1,2,\ldots,n_i, \tag{1.7}$$

where Φ denotes the numerical flux function, and $W^l_{i,j}$ and $W^r_{i,j}$ the constant state at the left and right side of $\partial \bar{C}_{i,j}$, respectively. The flux evaluation, and so the space discretization, may be either first- or higher-order accurate. First-order accuracy is obtained in the standard way: at each finite volume wall, the left and right state to be inserted into the numerical flux function are taken equal to that in the corresponding adjacent volume. Second-order accuracy is obtained with a MUSCL-approach. For a description of the precise second-order MUSCL-approach applied here, we refer to [4].

1.3. Existing solution method

To solve system (1.7) we consider the general unsteady system

$$\frac{dW_i}{dt} = R_i, \quad i=1,2,\ldots,n_i. \tag{1.8}$$

The natural choice for R_i is

$$R_i = \frac{-1}{A_i} \sum_{j=1}^{n_{ij}} T(\bar{n}_x,\bar{n}_y)_{i,j}\, \Phi(W^l_{i,j}, W^r_{i,j})\, \bar{l}_{i,j}, \tag{1.9}$$

where A_i is the area of finite volume C_i.

To have an upwind analogue to Jameson's central method [6], in [10] an explicit four-stage Runge-Kutta (RK4) scheme is applied for the temporal discretization of (1.8) with (1.9) as right-hand side. The benefits of the upwind analogue are evident: better shock capturing, greater robustness and no tuning of explicitly added artificial viscosity. Just as in [6], multigrid is applied for accelerating the solution process [11]. Given the upwind discretization, in [10] the Runge-Kutta coefficients are optimized for having both good stability and smoothing properties. Concerning computational efficiency, it seems that the upwind method is already competitive with Jameson's method, without introducing a further acceleration technique such as e.g. residual averaging. Interesting now is that the upwind analogue still allows another, straightforward efficiency improvement by exploiting the direct availability of the corresponding first-order upwind discretization with its better stability and smoothing properties. (We notice that since a first-order central discretization is not directly available, Jameson's method does not directly allow this improvement.)

2. New solution method

2.1. Explicit time stepping

Compared with the existing solution method, the new solution method only uses a more extensive right-hand side in the explicit time stepping scheme. The existing right-hand side is extended with two first-order upwind defects, one which is evaluated at each intermediate step of the multistage scheme and another which is kept frozen at the old time level and compensated for the other first-order defect by adding it to the right-hand side with the opposite sign. Further - which is most important - the second-order defect is kept frozen as well. Writing the four-stage time stepping scheme as

$$W_i^{n,k} = W_i^{n,0} + \Delta t_i \, \alpha_k \, R_i^{n,k-1}, \quad i = 1,2, \ldots, n_i, \; k = 1,2,3,4, \tag{2.1}$$

where n denotes the time level, k the intermediate time level, Δt_i the local time step and α_k the Runge-Kutta coefficients, for the existing method's right-hand side $R_i^{n,k-1}$ we can write

$$R_i^{n,k-1} = \frac{-1}{A_i} \sum_{j=1}^{n_{ij}} T(\bar{n}_x, \bar{n}_y)_{i,j} \, \Phi((W_{i,j}^l)^{n,k-1}, (W_{i,j}^r)^{n,k-1}) \bar{l}_{i,j}, \tag{2.2}$$

with $(W_{i,j}^l)^{n,k-1}$ and $(W_{i,j}^r)^{n,k-1}$ second-order accurate. For the new method now we have

$$\begin{aligned} R_i^{n,k-1} = \frac{-1}{A_i} \sum_{j=1}^{n_{ij}} T(\bar{n}_x, \bar{n}_y)_{i,j} \{ & \Phi(W_i^{n,k-1}, W_{i,j}^{n,k-1}) - \\ & \Phi(W_i^{n,0}, W_{i,j}^{n,0}) + \\ & \Phi((W_{i,j}^l)^{n,0}, (W_{i,j}^r)^{n,0}) \} \bar{l}_{i,j}, \end{aligned} \tag{2.3}$$

where only $(W_{i,j}^l)^{n,0}$ and $(W_{i,j}^r)^{n,0}$ are second-order accurate.

The new method proposed is of iterative defect correction (IDeC) type [2]. The second-order defect is evaluated on the finest grid only, using the finite element discretization existing there. Though introducing defect correction iteration in a pseudo-unsteady solution method is not as necessary as is the case for a pure relaxation method [7,8], it may lead to an improved efficiency and thus be useful. In section 3 we will show that the defect correction method proposed here can take advantage of a greater stability (larger local time steps) guaranteed by the first-order defects in the right-hand side. Further we will show that with multigrid as an acceleration technique, advantage can also be taken of better smoothing properties.

2.2. Multigrid and defect correction

The solution method can be divided into two successive stages. The first stage is nested iteration (full multigrid) which is applied to obtain a good initial solution on the finest grid. The second stage is the defect correction iteration which is used to iterate until a second-order accurate solution is obtained. The first iterate for the defect correction process is the solution obtained by nested iteration. The building block of both stages is nonlinear multigrid (full approximation scheme).

2.2.1. Nested iteration. To apply multigrid we construct a nested set of grids. For a description of the coarsening rule applied, we refer to [11]. Let $\Omega_1, \Omega_2, \ldots, \Omega_L$ be a sequence of nested grids with Ω_1 the coarsest and Ω_L the finest grid. The nested iteration starts with a user-defined initial estimate of W_1; the solution on the coarsest grid Ω_1. To obtain an initial solution on Ω_2, first the solution on Ω_1 is improved by a few nonlinear multigrid cycles (section 2.2.3). (The number of cycles used at each nested iteration step can be either fixed or dependent of the residual.) After this, the improved solution W_1 is prolongated to Ω_2. The process is repeated until Ω_L is reached.

The prolongation of the solution can be the simple piecewise constant prolongation $I^l_{l-1}, 2 \leqslant l \leqslant L$ as to be applied for prolongating the correction in nonlinear multigrid, or it can be a smoother one defined by

$$(\mathcal{I}^l_{l-1}(W_{l-1}))_i \equiv \frac{A_i(I^l_{l-1}(W_{l-1}))_i + \sum_{j=1}^{n_{i,j}} A_{i,j}(I^l_{l-1}(W_{l-1}))_{i,j}}{A_i + \sum_{j=1}^{n_{i,j}} A_{i,j}}, \quad 2 \leqslant l \leqslant L. \tag{2.4}$$

We notice that since I^l_{l-1} strictly obeys the physical conservation laws by prolongating cell-integrated amounts of mass, momentum and energy, $\mathcal{I}^l_{l-1}$ is strictly conservative also.

2.2.2. Defect correction. Let $\mathcal{F}^1_L(W_L)=0$ and $\mathcal{F}^2_L(W_L)=0$ denote the first-order respectively second-order discretized Euler equations on the finest grid. Then, defect correction iteration can be written as

$$\mathcal{F}^1_L(W^n_L) = \mathcal{F}^1_L(W^{n-1}_L) - \mathcal{F}^2_L(W^{n-1}_l), \quad n = 1,2, \ldots, n_d, \tag{2.5}$$

where W^0_L is the solution yielded by nested iteration. For smooth problems, a single IDeC-cycle is sufficient to obtain second-order accuracy [5]. For problems with discontinuities, experiments have shown that only a few IDeC-cycles significantly improve the accuracy of the solution [7]. For each IDeC-cycle we have to solve a first-order system with an appropriate right-hand side. From [7] it is known that it is inefficient to solve this system very accurately. There, with a steady approach, application of only a single nonlinear multigrid cycle per IDeC-cycle appears to be the most efficient strategy. Here, with our unsteady approach, we will re-investigate what is the optimal number of multigrid cycles per IDeC-cycle.

2.2.3. Nonlinear multigrid. A single nonlinear multigrid cycle is recursively defined in the following way:

(i) Improve on the starting grid Ω_l, $1 \leqslant l \leqslant L$, the latest obtained solution by applying ν_{pre} RK4-steps to

$$\mathcal{F}^1_l(W_l) = R_l. \tag{2.6}$$

(In the nested iteration stage we have on a finest grid Ω_l, $1 \leqslant l \leqslant L : R_l = 0$. In the defect correction stage we have on the finest grid $\Omega_L : R_L = \mathcal{F}^1_L(W_L) - \mathcal{F}^2_L(W_L)$.)

(ii) Approximate on the underlying coarse grid the solution of

$$\mathcal{F}^1_{l-1}(I^{l-1}_l(W_l)) = \mathcal{F}^1_{l-1}(I^{l-1}_l(W_l)) - \tilde{I}^{l-1}_l(\mathcal{F}^1_l(W_l) - R_l), \tag{2.7}$$

by applying a single nonlinear multigrid cycle. Notice that in the RK4-scheme the complete

right-hand side of (2.7) is kept frozen. The restriction operator I_l^{l-1} is such that it also exactly obeys the conservation of cell-integrated mass, momentum and energy. The restriction operator I_l^{l-1} restricts the defect in the standard way: by summation of mass, momentum and energy defects over fine grid cells that are to be grouped.

(iii) Improve the solution on Ω_l by correcting the current solution:

$$W_l = W_l + I_{l-1}^{l}(\Delta W_{l-1}), \tag{2.8}$$

where I_{l-1}^{l} is the piecewise constant prolongation operator, and by applying ν_{post} RK4-steps to (2.6).

3. Results

3.1. Analysis

To analyze the convergence properties of the iterative defect correction method proposed, we consider the unsteady 1D model equation

$$\frac{\partial w}{\partial t} + c\frac{\partial w}{\partial x} = 0, \quad c>0. \tag{3.1}$$

For the spatial discretization we consider a grid with a uniformly constant mesh size h. For the first-order upwind spatial discretization we have

$$\frac{\partial w}{\partial x} = \frac{-w_{i-1}+w_i}{h} + O(h). \tag{3.2}$$

As a second-order upwind discretization we take the Fromm scheme (i.e. van Leer's κ-scheme [13] with $\kappa=0$), which leads to

$$\frac{\partial w}{\partial x} = \frac{w_{i-2}-5w_{i-1}+3w_i+w_{i+1}}{4h} + O(h^2). \tag{3.3}$$

For both spatial discretizations and the existing explicit method, in [10] the following optimal Runge-Kutta coefficients are found: $\alpha_1=0.11$, $\alpha_2=0.2767$, $\alpha_3=0.5$. (Consistency requires: $\alpha_4=1.$) The optimization can be redone for the defect correction method. However, simply omitting the optimization, in the next section we will show that with the optimal α_k's found for the existing second-order method, defect correction already yields a better stability and smoothing.

3.1.1. Stability analysis. We will first perform a stability analysis for iterative defect correction with an explicit RK4-scheme as inner solution method. For this we consider the linear system

$$AW = b, \tag{3.4}$$

and the two operators A^1 and A^2, resulting from the first-order accurate and second-order accurate spatial discretization of (3.1), respectively. To solve the second-order system

$$A^2 W = b, \tag{3.5}$$

we apply the IDeC-process

$$A^1 W^0 = b, \tag{3.6a}$$

$$A^1 W^n = A^1 W^{n-1} + (b - A^2 W^{n-1}), \quad n=1,2,\ldots,n_d. \tag{3.6b}$$

Assuming A^1 to be invertible, the corresponding amplification matrix G reads

$$G = I - (A^1)^{-1}A^2. \tag{3.7}$$

Instead of solving each W^n from (3.6b) exactly, we approximate it by means of an explicit RK4-scheme. With ν the number of RK4-steps which allows us to define an (approximate) solution W^n,

we will now investigate how the corresponding amplification matrix G_ν is related to the amplification matrix G that corresponds with the exact solution of W^n from (3.6b). Denoting the approximate solution after ν RK4-steps as $W^{n,\nu}$, for $\nu=1$ we have

$$W^{n,1} = \{P+Q(A^1-A^2)\}W^{n-1}+Qb, \tag{3.8}$$

with

$$P = I-\Delta tA^1(I-\Delta t\alpha_3A^1(I-\Delta t\alpha_2A^1(I-\Delta t\alpha_1A^1))), \tag{3.9a}$$

$$Q = \Delta t(I-\Delta t\alpha_3A^1(I-\Delta t\alpha_2A^1(I-\Delta t\alpha_1A^1))). \tag{3.9b}$$

Hence, for G_1 we can write

$$G_1 = P+Q(A^1-A^2). \tag{3.10}$$

For $\nu>1$, one can easily find the recurrent relation

$$G_\nu = PG_{\nu-1}+Q(A^1-A^2), \tag{3.11}$$

which leads to

$$G_\nu = (I+P+P^2+\cdots+P^{\nu-1})Q(A^1-A^2)+P^\nu. \tag{3.12}$$

THEOREM. Let $\|\ .\ \|$ be some matrix norm. If $I-P$ is invertible and if $\|P\|<1$, then $\lim_{\nu\to\infty} G_\nu = G$.

PROOF. If $I-P$ is invertible, then for all $\nu>1$: $I+P+P^2+\cdots+P^{\nu-1} = (I-P)^{-1}(I-P^\nu)$.
If $\|P\|<1$, then $\lim_{\nu\to\infty}(I-P)^{-1}(I-P^\nu) = (I-P)^{-1}$.
Hence, $\lim_{\nu\to\infty} G_\nu = (I-P)^{-1}Q(A^1-A^2) = (A^1Q)^{-1}Q(A^1-A^2) =$
$(A^1)^{-1}Q^{-1}Q(A^1-A^2) = G$. □

Local mode analysis applied to (3.1) with A^1 and A^2 corresponding with (3.2) and (3.3), respectively, yields then for the maximally allowable value of $\sigma \equiv c\Delta t/\Delta x$: $\sigma_{\nu=1} = 2.21$ and $\sigma_{\lim \nu\to\infty} = 2.12$. Notice that the difference between both values is very small. For an arbitrary ν it is safe and still efficient to take $\sigma = 2.12$. The value $\sigma = 2.12$ is lower than that for the existing method applied to the first-order upwind system ($\sigma = 2.5105$, [9]), but higher than that for the existing method applied to the second-order ($\kappa=0$) system ($\sigma = 1.9186$, [9]).

For $\sigma = 2.12$ and increasing ν, we show in Fig. 1 the behaviour of the convergence factor $|\mu|$ versus the frequency θ in the range $[0,\pi]$. Already for $\nu = 1$, it appears that the convergence behaviour is better than that for the existing second-order method (Fig. 2.27 in [9]). Clearly visible for increasing ν is the rapid improvement of the smoothing (i.e. the convergence in the range $\theta\in[\pi/2,\pi]$), and the getting coincident of the curves. The curves converge to that corresponding with the exact solution of (3.6b): $|\mu| = \frac{1}{2}\sin(\theta)$, $\theta\in[0,\pi]$.

3.1.2. Smoothing analysis. Local mode analysis yields that with the new method optimal smoothing of the highest frequency, $\theta = \pi$, is obtained for $\sigma=1.8921$ and $\sigma=1.4869$. Similar to $\sigma = 2.12$ (Fig. 1), for $\sigma=1.8921$ and $\sigma=1.4869$ we show in Fig. 2 and Fig. 3, respectively, the convergence behaviour with increasing ν. For both values of σ the smoothing is clearly better than for $\sigma=2.12$. For $\sigma=1.4869$ the smoothing clearly is the best.

In Fig. 4,5 and 6 we show the smoothing behaviour for varying σ, the θ-range considered being $[\pi/2,\pi]$, and the quantity $|\mu|$ along the vertical axis being the maximum smoothing factor found over this range. Considered are successively: the first-order method (Fig. 4), the old second-order method (Fig. 5) and the new second-order method (Fig. 6). Comparing the results of the old and new second-order method, it clearly appears that the latter has better smoothing properties. Notice that in particular the σ-range over which its smoothing is good is much wider.

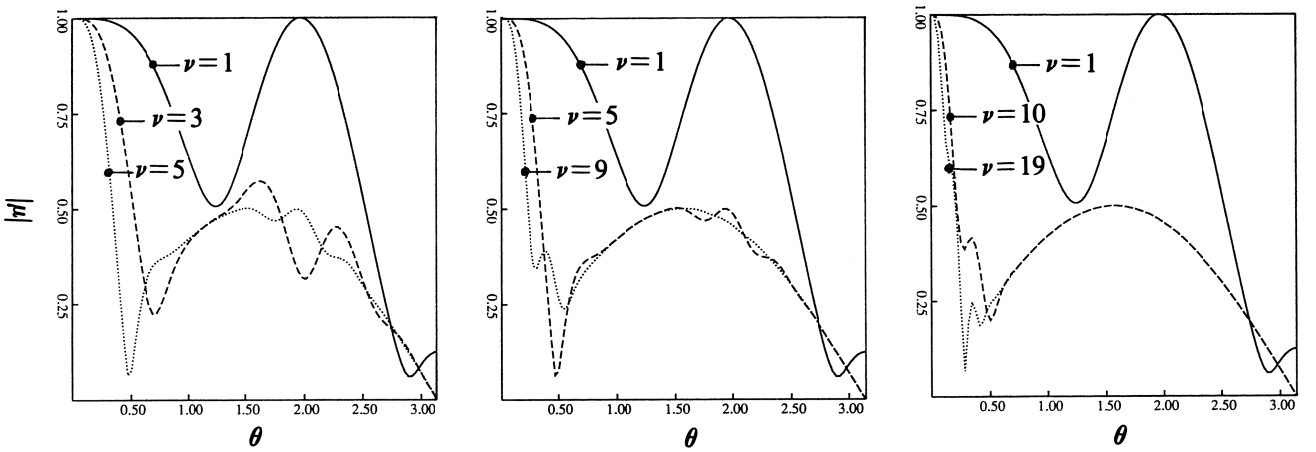

a. $\nu=1,3,5.$ b. $\nu=1,5,9.$ c. $\nu=1,10,19.$

Fig. 1. Convergence behaviour for $\sigma=2.12$.

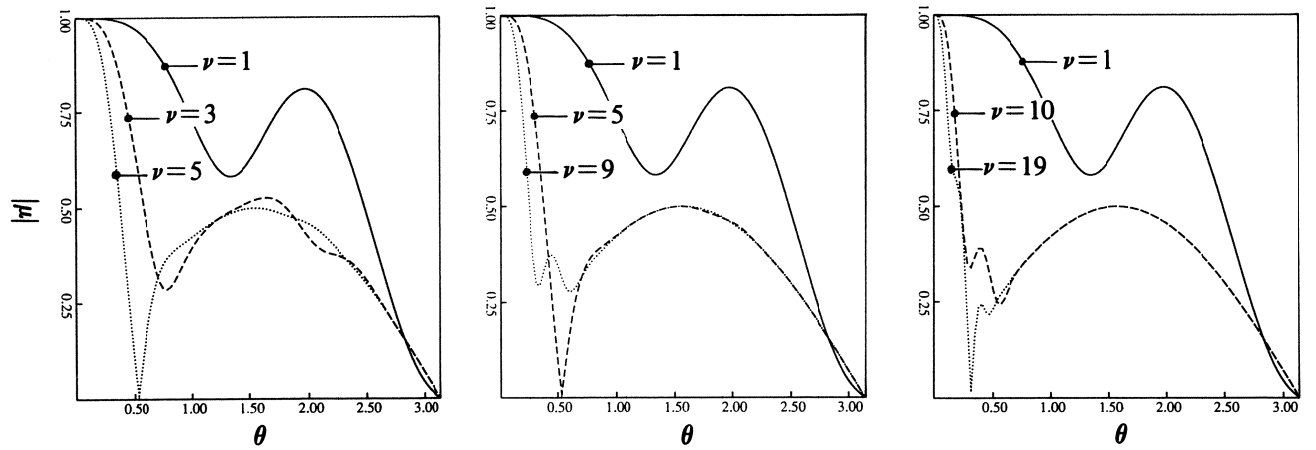

a. $\nu=1,3,5.$ b. $\nu=1,5,9.$ c. $\nu=1,10,19.$

Fig. 2. Convergence behaviour for $\sigma=1.8921$.

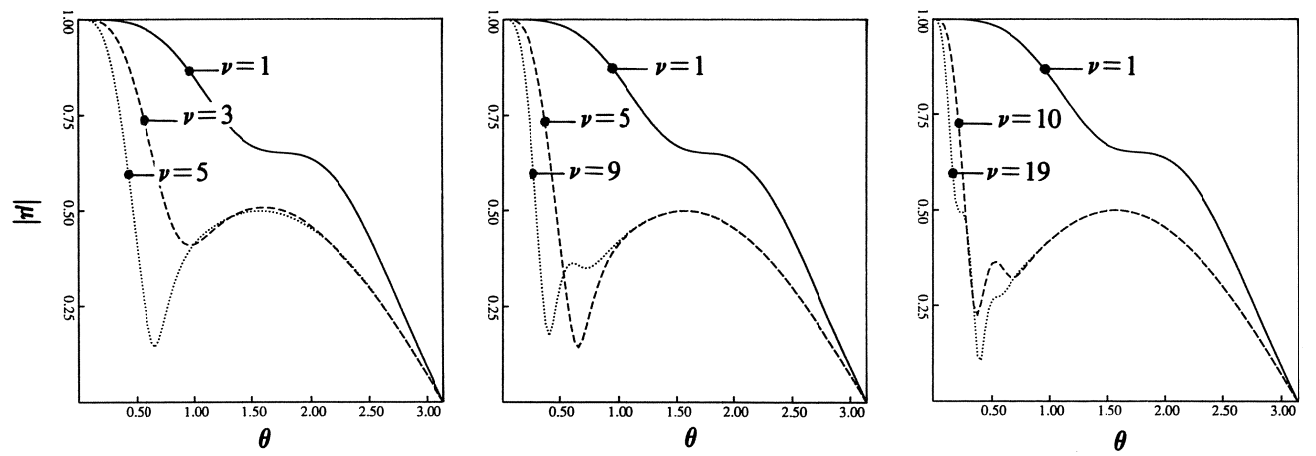

a. $\nu=1,3,5.$ b. $\nu=1,5,9.$ c. $\nu=1,10,19.$

Fig. 3. Convergence behaviour for $\sigma=1.4869$.

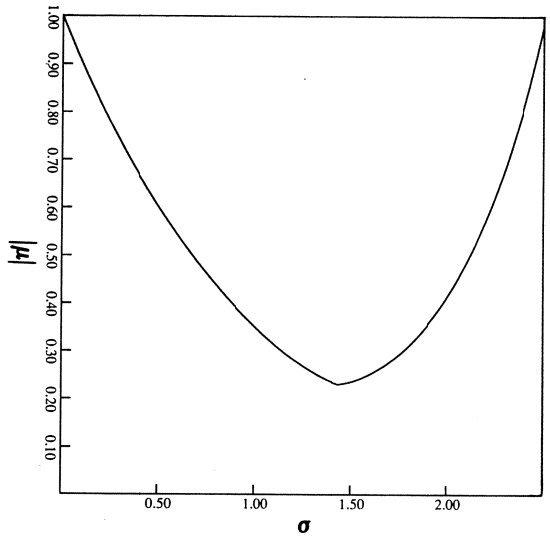

Fig. 4. Smoothing behaviour for varying σ, first-order method.

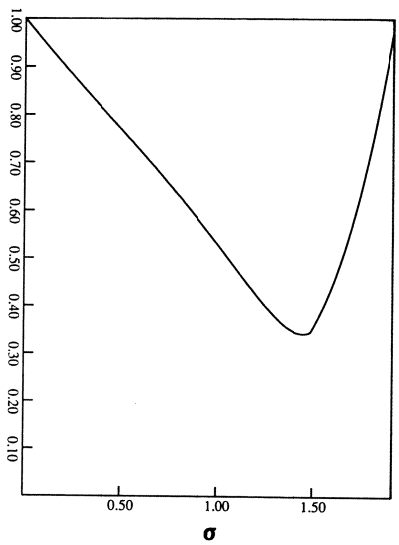

Fig. 5. Smoothing behaviour for varying σ, old second-order method.

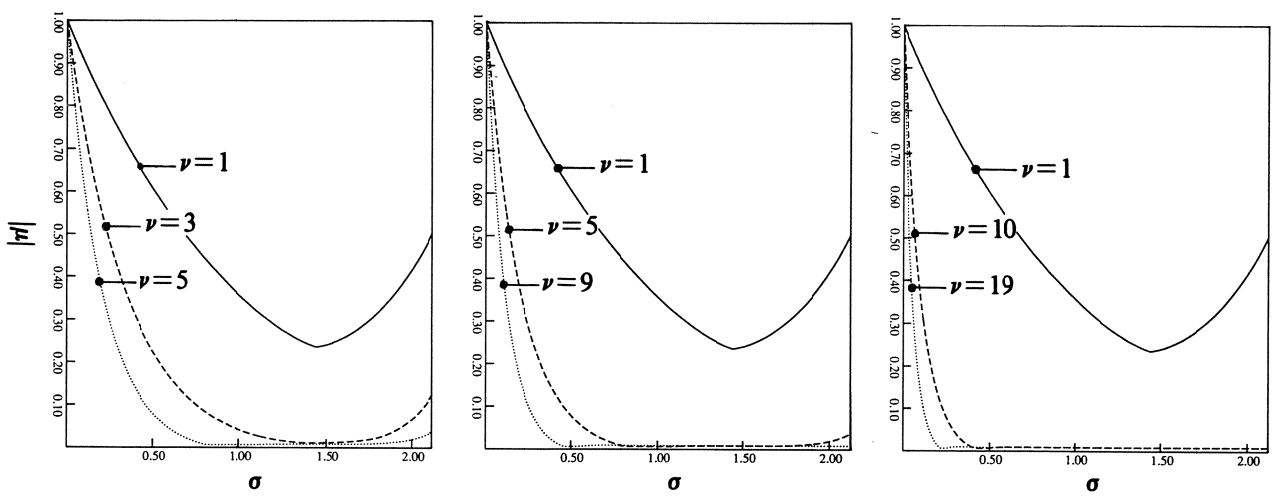

a. $\nu=1,3,5$.

b. $\nu=1,5,9$.

c. $\nu=1,10,19$.

Fig. 6. Smoothing behaviour for varying σ, new second-order method.

3.2. Experiments

To verify the previously predicted better stability and convergence properties of iterative defect correction, we consider the standard transonic channel flow from [15].

As finest grid we apply the 161-cells grid given in Fig. 4.1 of [9]. The multigrid strategy applied is a 4-level strategy, each multigrid cycle being a V-cycle with $\nu_{pre} = \nu_{post} = 1$, $\forall l$. On all coarser grids we apply the first-order scheme only. Convergence results for the old second-order method are given in Fig. 7 and Tab. 1. (Notice that Fig. 7 and all similar convergence graphs in this paper start at the very beginning of the solution process; the beginning of the nested iteration.) In Tab. 1, a denotes the convergence factor per multigrid cycle, n the total number of multigrid cycles (starting from Ω_L) that are required for obtaining a fixed residual reduction, and t the computing time measured on a Convex-C2. Similar convergence results for the new second-order method are given in Fig. 8 and Tab. 2 for successively $\nu_{FAS} = 1,2,5$ and 10, ν_{FAS} denoting the number of multigrid cycles per IDeC-cycle. Notice that, in agreement with the theoretical results just obtained, the convergence rate increases with decreasing ν_{FAS}, but the efficiency decreases. The most efficient strategy is obtained for $\nu_{FAS} = 1$. Comparison of the new method's efficiency with that of the old second-order method shows that, for $\nu_{FAS} = 1$, the new method is significantly more efficient than the old method.

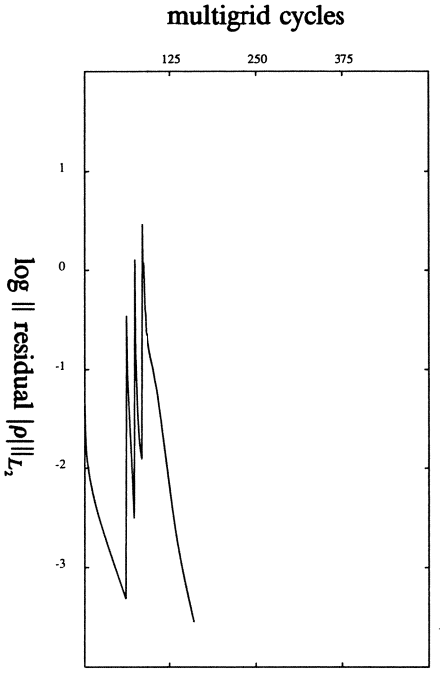

Fig. 7. Convergence history 161-cells problem, old second-order method.

a	n_d	t (sec)
0.8853	77	187.6

Tab. 1. Performance old second-order method (161-cells problem).

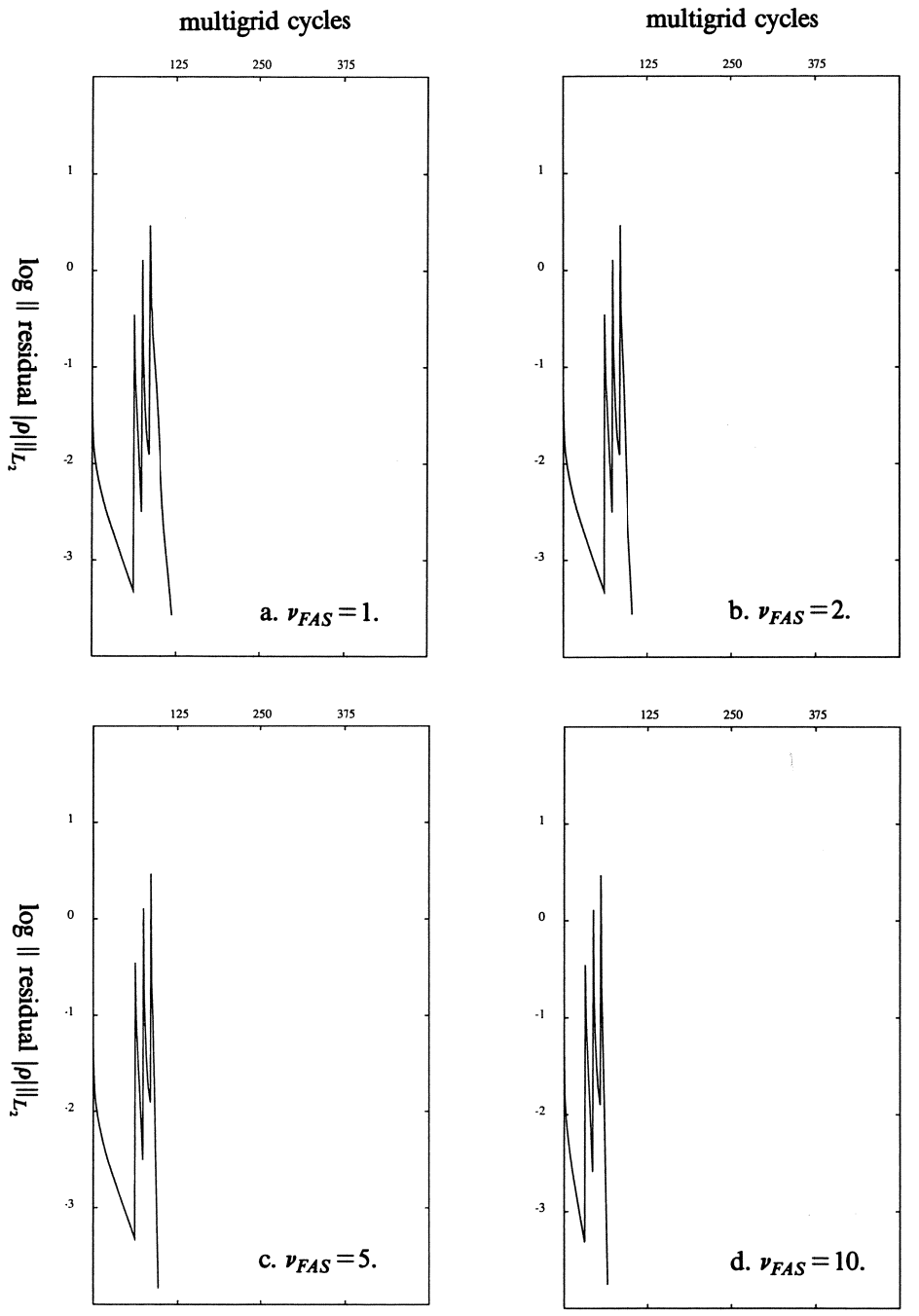

Fig. 8. Convergence history 161-cells problem, new second-order method.

a	n_d	t (*sec*)
0.7664	36	73.4
0.6139	20	80.7
0.4063	12	104.5
0.3784	11	174.9

Tab. 2. Performance new second-order method (161-cells problem).

In Fig. 9 and Tab. 3 we present the convergence results for a 5-level strategy with a finer finest grid (the 585-cells grid also given in Fig. 4.1 of [9]) and with $\nu_{FAS} = 10$. Notice that the convergence rate is about the same as that for the previously considered coarser $\nu_{FAS} = 10$-case (Fig. 8d and Tab. 2). The convergence rate of IDeC seems to be independent of the number of grid cells. The observed grid independence is supported by a study made by Désidéri [3] on the convergence of solution methods for second-order systems, using a first-order preconditioning. (The study referred to yields $(½)^n$ as asymptotic convergence rate, with n denoting the total number of iterations performed; in our case the number of IDeC-cycles n_d, which in our case also is the number of multigrid cycles starting from Ω_L.)

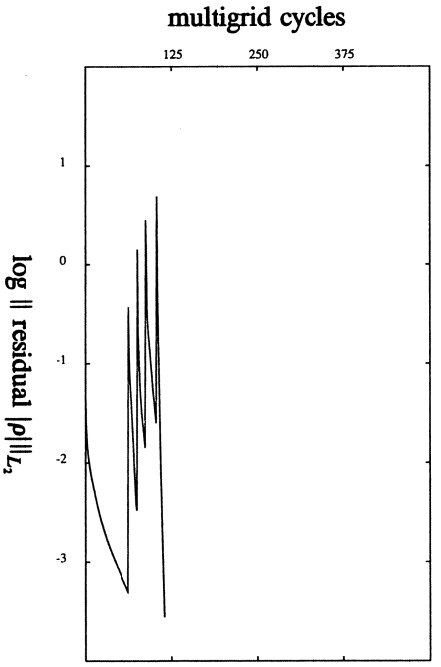

Fig. 9. Convergence history 585-cells problem, new second-order method ($\nu_{FAS} = 10$).

a	n_d	t (*sec*)
0.4106	12	748.2

Tab. 3. Performance new second-order method (585-cells problem).

4. Conclusions

Fully implicit solution methods may strongly benefit from defect correction iteration when the system(s) of discretized equations are not diagonally dominant, as may be the case with higher-order accurate discretizations. Fully explicit solution methods now may also profit from defect correction iteration. Here, the profits are faster convergence and higher efficiency. The defect correction method appears to be more stable (and hence more robust) than the old (standard) explicit method. Compared to the old explicit method it possesses remarkably good smoothing properties, in fact even better than the first-order method (compare Fig. 4 and 6). Last but not least its convergence rate seems to be grid-independent. For upwind discretizations, the 'price' that has to be paid for using defect correction iteration - a more complex algorithm - is negligible. This because of the direct availability of an appropriate approximate operator; the first-order upwind operator.

References

1. K. Baba and M. Tabata, *On a Conservative Upwind Finite Element Scheme for Convective Diffusion Equations*, RAIRO Numer. Anal. 15, 3-25 (1981).
2. K Böhmer, P.W. Hemker and H.J. Stetter, *The Defect Correction Approach*, Computing Suppl. 5, 1-32 (1984).
3. J.A. Désidéri, *Preliminary Results on the Iterative Convergence of a Class of Implicit Schemes*, Institut National de Recherche en Informatique et en Automatique, Sophia-Antipolis, Report 490 (unpublished, 1986).
4. F. Fézoui, *Résolution des Equations d'Euler par un Schéma de van Leer en Eléments Finis*, Institut National de Recherche en Informatique et en Automatique, Sophia-Antipolis, Report 358 (unpublished, 1985).
5. W. Hackbusch, *Multi-Grid Methods and Applications*, Springer, Berlin (1985).
6. A. Jameson, *Solution of the Euler Equations for Two Dimensional Transonic Flow by a Multigrid Method*, Appl. Math. Comput. 13, 327-355 (1983).
7. B. Koren, *Defect Correction and Multigrid for an Efficient and Accurate Computation of Airfoil Flows*, J. Comput. Phys. 77, 183-206 (1988).
8. B. Koren, *Multigrid and Defect Correction for the Steady Navier-Stokes Equations*, J. Comput. Phys. (accepted for publication).
9. M-H. Lallemand, *Schémas Décentrés Multigrilles pour la Résolution des Equations d'Euler en Eléments Finis*, Thèse de Docteur, Université de Provence, Centre Saint Charles (Institut National de Recherche en Informatique et en Automatique, Sophia-Antipolis (1988).
10. M-H. Lallemand, *Dissipative Properties of Runge-Kutta Schemes with Upwind Spatial Approximation for the Euler Equations*, Institut National de Recherche en Informatique et en Automatique, Sophia-Antipolis (to appear).
11. M-H. Lallemand and A. Dervieux, *A Multigrid Finite Element Method for Solving the Two-Dimensional Euler Equations*, in Multigrid Methods, Theory, Applications, and Supercomputing, Proceedings of the Third Copper Mountain Conference on Multigrid Methods, Copper Mountain, 1987, Lecture Notes in Pure and Applied Mathematics Vol. 110, 337-363, edited by S.F. McCormick (Dekker, New York, 1988).
12. B. van Leer, *Flux-Vector Splitting for the Euler Equations*, in Proceedings of the Eighth International Conference on Numerical Methods in Fluid Dynamics, Aachen, 1982, Lecture Notes in Physics Vol. 170, 507-512, edited by E. Krause (Springer, Berlin, 1982).
13. B. van Leer, *Upwind-Difference Methods for Aerodynamic Problems Governed by the Euler Equations*, in Large Scale Computations in Fluid Mechanics, Proceedings of the 15th AMS-SIAM Summer Seminar on Applied Mathematics, Scripps Institution of Oceanography, 1983, Lectures in Applied Mathematics Vol. 22, Part 2, 327-336, edited by B.E. Engquist et al. (Amer. Math. Soc., Providence, RI, 1985).
14. S. Osher and F. Solomon, *Upwind-Difference Schemes for Hyperbolic Systems of Conservation Laws*, Math. Comput. 38, 339-374 (1982).
15. A. Rizzi and H. Viviand, *Numerical Methods for the Computation of Inviscid Transonic Flows with Shock Waves*, Notes on Numerical Fluid Mechanics Vol. 3 (Vieweg, Braunschweig, 1981).
16. P.L. Roe, *Approximate Riemann Solvers, Parameter Vectors and Difference Schemes*, J. Comput. Phys. 43, 357-372 (1981).
17. J.L. Steger and R.F. Warming, *Flux Vector Splitting of the Inviscid Gas Dynamics Equations with Applications to Finite Difference Methods*, J. Comput. Phys. 40, 263-293 (1981).